Reactivity of Sulfur Molecules on MoO₃ (010) Surface
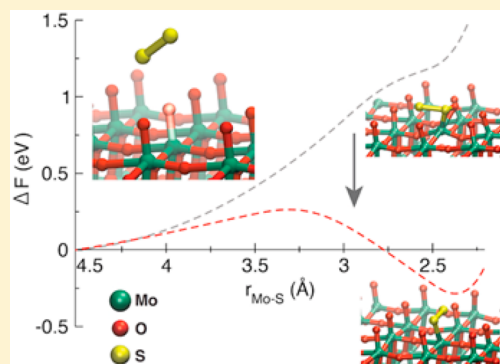
Masaaki Misawa,[†,‡] Subodh Tiwari,[†] Sungwook Hong,[†] Aravind Krishnamoorthy,[†] Fuyuki Shimojo,[‡] Rajiv K. Kalia,[†] Aiichiro Nakano,[†] and Priya Vashishta*,[†]

[†]Collaboratory for Advanced Computing and Simulations, Department of Physics & Astronomy, Department of Computer Science, Department of Chemical Engineering & Materials Science, Department of Biological Sciences, University of Southern California, Los Angeles, California 90089-0242, United States

[‡]Department of Physics, Kumamoto University, Kumamoto 860-8555, Japan

S *Supporting Information*

ABSTRACT: Two-dimensional and layered MoS₂ is a promising candidate for next-generation electric devices due to its unique electronic, optical, and chemical properties. Chemical vapor deposition (CVD) is the most effective way to synthesize MoS₂ monolayer on a target substrate. During CVD synthesis, sulfidation of MoO₃ surface is a critical reaction step, which converts MoO₃ to MoS₂. However, initial reaction steps for the sulfidation of MoO₃ remain to be fully understood. Here, we report first-principles quantum molecular dynamics (QMD) simulations for the initiation dynamics of sulfidation of MoO₃ (010) surface using S₂ and S₈ molecules. We found that S₂ molecule is much more reactive on the MoO₃ surface than S₈ molecule. Furthermore, our QMD simulations revealed that a surface O-vacancy on the MoO₃ surface makes the sulfidation process preferable kinetically and thermodynamically. Our work clarifies an essential role of surface defects to initiate and accelerate the reaction of MoO₃ and gas-phase sulfur precursors for CVD synthesis of MoS₂ layers.

Two-dimensional and layered transition metal dichalcogenides (TMDCs) are attracting great attention for functional semiconducting materials because of their unique electric and optoelectronic properties.[1−7] Among possible layered TMDCs materials in nature, MoS₂ monolayer has been considered a promising candidate for next-generation electronic devices primarily due to its higher carrier mobility[8,9] and a layer-dependent direct band gap (e.g., 1.29 eV − 1.8 eV).[10,11] To bring such an interesting MoS₂ layer into mass production for semiconducting nanostructures, recent progress has been made in developing synthesis techniques for high-quality MoS₂ layers, which includes mechanical exfoliation, physical vapor deposition, and chemical vapor deposition (CVD).[3,12]

Among these techniques, CVD is the most practical method to synthesize atomically thin MoS₂ layers with high continuity and uniformity.[13−15] In a typical CVD process, MoO₃ reactants and sulfur powders are generally used,[16−18] and they react with each other at elevated temperatures to form mono/few MoS₂ layers on substrates. Thus, it is essential to understand basic reaction processes for sulfidation of MoO₃. Theses elementary sulfidation steps of MoO₃ have been studied and understood by both experimental and theoretical work: Weber et al.[19] conducted the sulfidation of crystalline MoO₃ with H₂S/H₂ gas to understand reaction mechanisms by using X-ray photoelectron and infrared emission spectroscopy, and suggested that the conversion of terminal Mo = Oₜ to Mo = S is the key reaction of the sulfidation process. Kumar et al.[20]

found that MoO₃ precursors were reduced by both H₂ gas and sulfur precursors, and then, O atoms were further replaced by S atoms, leading to the sulfidation of MoO₃ to MoS₂. Similar results were reported by Shi et al.[21] who conducted extensive density functional theory studies for elementary processes of sulfidation of MoO₃ surfaces. They suggested that sulfur substitution on the MoO₃ surface could favorably occur at O-termination sites, and the sulfidation process could be accelerated by the existence of surface O-vacancy.

However, fundamental understanding of reactivity of sulfur precursors on MoO₃ surfaces has yet to be achieved. Dynamics and energetic information on the sulfidation of MoO₃ with the presence of surface O-vacancy has also remained unclear. Atomic-scale modeling and simulations provide valuable insights into dynamic behaviors of surface-gas interfaces at atomic-length scales.[22] Here, we perform first-principles quantum molecular dynamics (QMD) simulations for reactions of MoO₃ surface and sulfur molecules to investigate the initial stage of the sulfidation process. QMD simulations follow the trajectories of all atoms while computing interatomic forces quantum mechanically from first-principles, allowing us to predict physical and chemical properties of complex materials.[23−25] In this work, we evaluate the reactivity of two sulfur

molecules, S_2 and S_8, on a MoO$_3$ (010) surface and discuss an essential role of surface O-vacancy in the sulfidation of MoO$_3$ surfaces.

To study the reactivity of sulfur molecules on the MoO$_3$ surface, we construct simulation cells that include a monolayered Mo$_{32}$O$_{96}$ structure (Figure 1a). The MoO$_3$
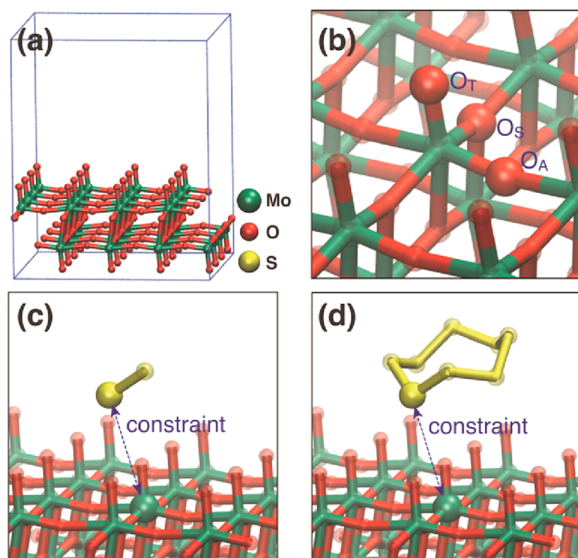

Figure 1. (a) The simulation cell that includes MoO$_3$ (010) surface. (b) The terminal (O$_T$), symmetric (O$_S$), and asymmetric (O$_A$) oxygen sites in crystalline MoO$_3$. (c,d) Simulation cells containing the MoO$_3$ (010) surface with S_2 and S_8 molecules, respectively. The interatomic distances between Mo and S atoms, exaggerated by larger spheres, are constrained during the QMD simulations.

surface has three nonequivalent oxygen sites: terminal (O$_T$),[5] asymmetric (O$_A$) and symmetric (O$_S$)[16] oxygen sites as shown in Figure 1b. The O$_T$ is bound to only one Mo, and exposed on the top or bottom surface. The O$_A$ and O$_S$ are located on the subsurface area of the MoO$_3$ substrate and connected with two and three Mo atoms, respectively. Those bond distances along the subsurface is asymmetric for O$_A$ and symmetric for O$_S$. For QMD simulations, we considered both S_2 and S_8 molecules as precursors. To reproduce the sulfidation reactions, an interatomic distance between Mo and S atoms (r_{Mo-S}) is constrained (Figure 1c,d), and we decreased the distance gradually during the simulations.

To investigate the sulfidation reactivity of the Mo atom in crystalline MoO$_3$, changes in the free energy (ΔF) during the QMD simulations were calculated by integrating Lagrange's multiplier $\lambda(r)$ along the constrained distance $r = r_{Mo-S}$:

$$\Delta F(r) = \int_{r_0}^{r} \langle \lambda(r') \rangle \, dr' \tag{1}$$

where the $\lambda(r)$ is obtained by averaging over the last 1000 steps of the QMD simulations for each r_{Mo-S}. When the period of r_{Mo-S} oscillations is too large during the 1000 steps, we performed additional QMD simulations up to 1500 steps for the same r_{Mo-S}. The Supporting Information includes further details in the ΔF calculations: The time evolution of λ and the average $\lambda(r)$ obtained from all of our calculations are shown in Figure S1. Figure S1a−d displays the time evolution of λ for MoO$_3$/S$_8$ systems without and with a surface O vacancy and for MoO$_3$/S$_2$ systems without and with a surface O vacancy,

respectively. The average $\lambda(r)$ without and with a surface O vacancy are shown in Figure S1e,f, respectively. The topics about the surface O vacancy will be described later.

The calculated ΔF changes and the corresponding QMD snapshots are shown in Figure 2a and Figure 2b−e,
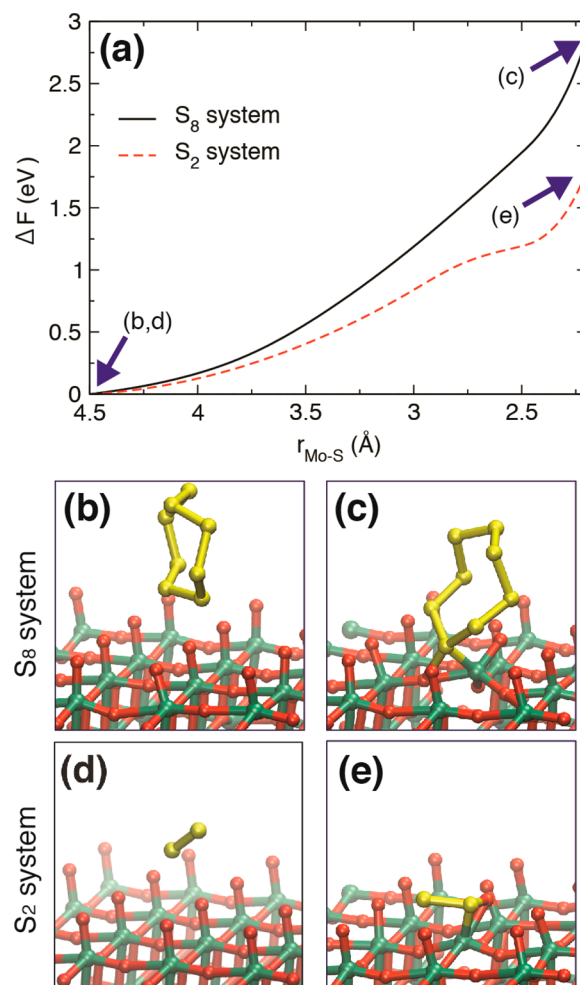

Figure 2. (a) Relative free energy versus r_{Mo-S} for S_8 (the black solid curve) and S_2 (the red dotted curve) systems on the intact MoO$_3$ surface. (b−e) Snapshots of the QMD simulations for S_8 (b,c) and for S_2 systems (d,e).

respectively. In both S_8 and S_2 systems, the initial r_{Mo-S} value was set to be 4.5 Å (Figure 2b,d), and it was found that the ΔF values increase monotonically while reducing r_{Mo-S}. In the final configuration, Mo−S bonds were formed due to the applied constrained force as shown in Figure 2c,e, but the MoO$_3$/S$_2$ and MoO$_3$/S$_8$ systems gained energy (i.e., endothermic) about 1.76 and 2.77 eV, respectively. This result explains that an intact MoO$_3$ (010) surface is unlikely to provide reactive sites to interact with S_8 or S_2 molecules, indicating that surface defects are necessary to activate the sulfidation reaction.

In the light of the observed nonreactivity of S_2 and S_8 molecules on a perfect MoO$_3$ surface, we performed additional QMD simulations by introducing a surface O-vacancy. Namely, we intentionally generated a surface defect by removing one O$_T$ atom on top of the MoO$_3$ substrate. After removing the O$_T$ atom, the surface geometry was optimized by using the quasi-Newton method.

It is interesting to note that during the optimization process, a surface modification around the defect was observed (Figure 3a−c). Namely, after removing the O atom in the O_T site
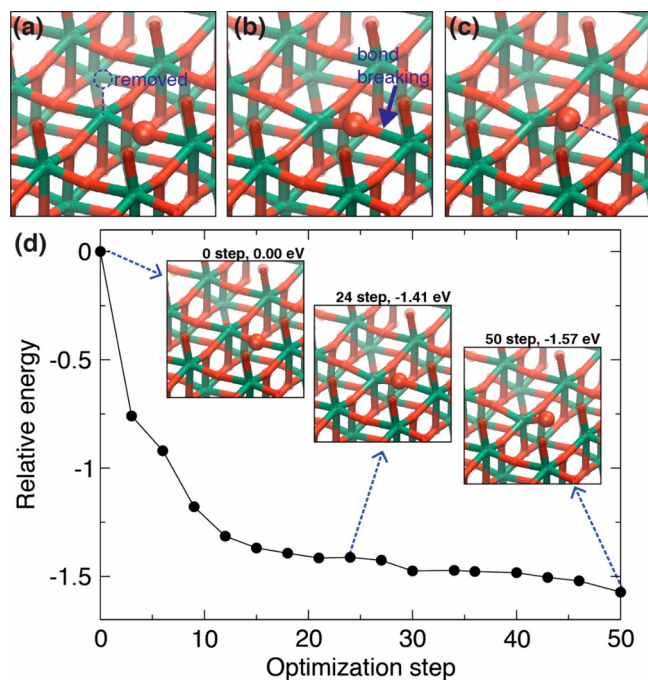

Figure 3. (a−c) Surface modification by O-vacancy formation during structural optimization: (a) Just after removing an O_T atom, (b) Mo−O_A bond breaking next to the O-vacancy, and (c) final relaxed structure. (d) Change in the potential energy during the structural optimization after introducing a surface O vacancy. Here, the potential energy is relative to that of the initial configuration.

(Figure 3a), an O atom in the neighboring O_A site moved upward (Figure 3b), and then, a Mo−O_A bond was broken (Figure 3c). As shown in Figure 3d, after 50 steps of the optimization process, potential energy of the final configuration was 1.57 eV lower than that of the initial configuration, confirming that the surface modification is an essential step after removing the O_T atom. Due to the surface modification, the defect structure became an O_A point-like vacancy rather than O_T vacancy. This atomic behavior could be explained by changes in Mo−O bond order at the vicinity of surface vacancies.[26]

After the surface modification, constrained QMD simulations were performed with a single S_8/S_2 molecule to investigate the sulfidation behavior of the MoO_3 surface with the O-vacancy. The ΔF curves for the MoO_3/S_8 and MoO_3/S_2 systems with the surface O-vacancy are shown in Figure 4a, and the corresponding QMD snapshots are described in Figure 4b−e. In these systems, the ΔF curves behaved quite differently from the intact MoO_3 surface systems. For the S_8 molecule, while the free energy kept increasing during the QMD simulations, the total energy gain is about 0.80 eV, which is much lower than the case of the intact MoO_3/S_8 system (2.77 eV). For the S_2 molecule, ΔF increased slightly and reached a maximum of 0.26 eV at $r_{Mo−S}$ = 3.25 Å. As the $r_{Mo−S}$ decreased further down to 2.4 Å, ΔF kept decreasing and reached a minimum of −0.25 eV (i.e., exothermic). This energetic data indicates that S_2 binding to the MoO_3 surface with the O vacancy is a thermodynamically and kinetically preferable reaction, i.e., Figure 4a shows that the entire reaction with the S_2 molecule is exothermic with
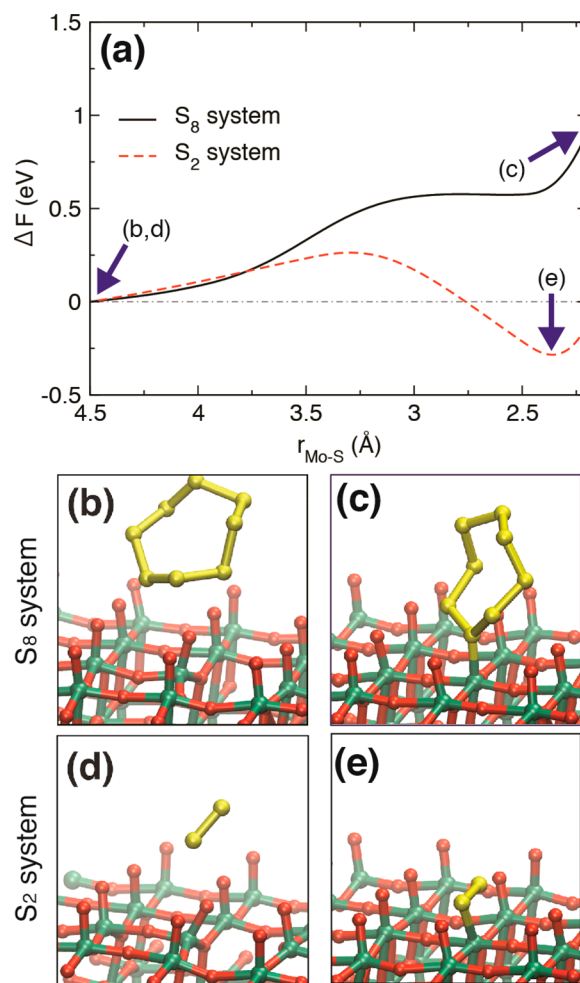

Figure 4. (a) Relative free energy versus $r_{Mo−S}$ for S_8 (the black solid curve) and S_2 (the red dotted curve) systems with the surface O-vacancy. (b−e) Snapshots of the QMD simulations (b,c) for S_8 and (d,e) for S_2 systems, with the corresponding $r_{Mo−S}$ values indicated in panel a.

a low activation barrier of $\Delta \sim 0.26$ eV. This leads to a rather fast kinetics at a typical growth temperature of T = 700 °C as

$$k = \frac{k_B T}{h} \exp\left(-\frac{\Delta}{k_B T}\right) \sim 8.8 \times 10^{11} \text{ s}^{-1} \qquad (2)$$

where, k_B, h, and Δ are the Boltzmann constant, plank constant, and corresponding activation barrier, respectively. Additionally, the final Mo−S interatomic distance is quantitatively consistent with a Mo−S bond distance in the crystalline MoS_2. In the final configuration, the S_8 and S_2 molecules nondissociatively chemisorbed on the O_T site (Figures 4c,e, respectively), while the O atom initially displaced upward (see Figure 3c) was pushed down to the asymmetric site by decreasing $r_{Mo−S}$. This is due to the surface remodification during the sulfidation reaction. Namely, during the constrained QMD simulations, the atomic position of the O atom, which moved upward from the O_A site, preferentially returned to the original position at $r_{Mo−S}$ = 3.0 Å due to the repulsion force between the S_8 or S_2 molecule and the O atom. Movie S1 in the Supporting Information shows the surface remodification process observed in the constrained QMD simulations for the MoO_3/S_2 system with a surface vacancy. After the O atoms returned to the

asymmetric site, the unconstraint S atom approached Mo atoms, leading to the formation of Mo−S bond. This fact also appears in the sign of the average interatomic force at r_{Mo-S} = 3.0 Å in S_2 with a vacancy system (see Figure S1f in the Supporting Information). As a result, we observed that the S_2 molecule preferentially oriented to the asymmetric axis of the crystalline MoO_3 at the final configuration. This adsorption formation is consistent with the adsorption mechanism proposed by Coquet et al.,[27] and is explained that the S_2^{2-} ligand are formed on the Mo atom proposed by Shi et al.[21] According to a computational work by Hong et al.,[28] it is expected that the S_2^{2-} ligand can be further dissociated, and then one of S atoms can diffuse to the neighboring O_T atom during the sulfidation process.

In conclusion, we performed QMD simulations of S_8 and S_2 on MoO_3 surface with constrained Mo−S interatomic distance to elucidate the initiation dynamics of sulfidation of MoO_3. We found that an S_8 molecule is inactive on both intact and defected MoO_3 surfaces. On the other hand, an S_2 molecule can favorably react with the surface O-vacancy on a MoO_3 surface. These results reveal that the surface defect structure can activate and accelerate the reactions of MoO_3 reactants and sulfur precursors. Therefore, our work suggests that the reducing agent to make structural defects such as H_2 gas plays an important role in CVD synthesis of MoS_2 layers.

Details of the QMD method are described in the Supporting Information. A simulation cell consists of a monolayered $Mo_{32}O_{96}$ structure with a side length of L_x = 15.850 Å, L_y = 19.387 Å, and L_z = 14.788 Å. A periodic boundary condition was applied to all directions. Vacuum region more than twice the thickness of the substrate was introduced in the yz-direction to avoid interactions between sulfur molecules with bottom side of the MoO_3 substrate. While a unit structure of crystalline MoO_3 has double layers connected by weak van der Waals interaction, the lower layer was not used in our simulation to reduce simulation costs. Atomic positions in the lower half of the MoO_3 substrate were frozen in our calculations in order to represent a bulk condition. The simulation cells were thermalized at 300 K with a time step of 1.21 fs using the canonical ensemble. The QMD simulations are performed up to 1500 steps (corresponding to 1.8 ps) for each r_{Mo-S} value.

It should be noted that various properties in crystalline MoO_3 are influenced by localized d-electrons of Mo atoms, and generalized gradient approximation (GGA)+U functional is commonly used to reproduce the on-site Coulomb interaction of those electrons.[29] However, GGA[30] functional was used in our QMD simulation instead. To validate that our conclusions regarding the initial steps of the sulfidation reaction are insensitive to this difference, we analyzed the energetic properties of S_2 adsorption process on MoO_3 surface by using the nudged elastic band (NEB) method.[31] The results of the NEB calculations confirmed that there is negligible difference in the reaction barrier and reaction energy between the GGA+U and GGA methods (Table S1 in the Supporting Information). Additionally, we tested the effects of spin-polarization on the reaction behaviors, since the ground state of an S_2 molecule is spin-triplet. Regarding this issue, we performed additional NEB calculations for GGA and GGA+U with spin-polarization. All of the NEB results show that the observations in our QMD simulations remain unchanged (Table S1 in the Supporting Information). Moreover, it was revealed that the spin-polarization of an S_2 molecule almost

vanishes after being adsorbed to an Mo atom (Figure S2 in the Supporting Information).

ASSOCIATED CONTENT

Ⓢ Supporting Information

The Supporting Information is available free of charge on the ACS Publications website at DOI: 10.1021/acs.jpclett.7b03011.

> QMD simulation methods and details (PDF)
> Movie S1: Surface remodification process observed in the constrained QMD simulations for the MoO_3/S_2 system with a surface vacancy (ZIP)

AUTHOR INFORMATION

Corresponding Author
*E-mail: priyav@usc.edu.

ORCID Ⓘ
Sungwook Hong: 0000-0003-3569-7701
Aravind Krishnamoorthy: 0000-0001-6778-2471
Aiichiro Nakano: 0000-0003-3228-3896
Priya Vashishta: 0000-0003-4683-429X

Notes
The authors declare no competing financial interest.

REFERENCES

(1) Gupta, A.; Sakthivel, T.; Seal, S. Recent development in 2D materials beyond graphene. *Prog. Mater. Sci.* 2015, 73, 44−126.

(2) Lee, Y. H.; Zhang, X. Q.; Zhang, W.; Chang, M. T.; Lin, C. T.; Chang, K. D.; Yu, Y. C.; Wang, J. T. W.; Chang, C. S.; Li, L. J.; et al. Synthesis of Large-Area MoS_2 Atomic Layers with Chemical Vapor Deposition. *Adv. Mater.* 2012, 24, 2320−2325.

(3) Venkata Subbaiah, Y.; Saji, K.; Tiwari, A. Atomically Thin MoS_2: A Versatile Nongraphene 2D Material. *Adv. Funct. Mater.* 2016, 26, 2046−2069.

(4) Lv, Z.; Mahmood, N.; Tahir, M.; Pan, L.; Zhang, X.; Zou, J.-J. Fabrication of zero to three dimensional nanostructured molybdenum sulfides and their electrochemical and photocatalytic applications. *Nanoscale* 2016, 8, 18250−18269.

(5) van der Zande, A. M.; Huang, P. Y.; Chenet, D. A.; Berkelbach, T. C.; You, Y.; Lee, G.-H.; Heinz, T. F.; Reichman, D. R.; Muller, D. A.; Hone, J. C. Grains and grain boundaries in highly crystalline monolayer molybdenum disulfide. *Nat. Mater.* 2013, 12, 554−561.

(6) Nourbakhsh, A.; Zubair, A.; Sajjad, R. N.; Amir Tavakkoli, K. G.; Chen, W.; Fang, S.; Ling, X.; Kong, J.; Dresselhaus, M. S.; Kaxiras, E.; et al. MoS_2 Field-Effect Transistor with Sub-10 nm Channel Length. *Nano Lett.* 2016, 16, 7798−7806.

(7) Ashton, M.; Paul, J.; Sinnott, S. B.; Hennig, R. G. Topology-Scaling Identification of Layered Solids and Stable Exfoliated 2D Materials. *Phys. Rev. Lett.* 2017, 118, 106101.

(8) Lembke, D.; Kis, A. Breakdown of high-performance monolayer MoS_2 transistors. *ACS Nano* 2012, 6, 10070−10075.

(9) Zhang, W.; Zhang, P.; Su, Z.; Wei, G. Synthesis and sensor applications of MoS_2-based nanocomposites. *Nanoscale* 2015, 7, 18364−18378.

(10) Mak, K. F.; Lee, C.; Hone, J.; Shan, J.; Heinz, T. F. Atomically thin MoS$_2$: a new direct-gap semiconductor. *Phys. Rev. Lett.* **2010**, *105*, 136805.

(11) Sundaram, R.; Engel, M.; Lombardo, A.; Krupke, R.; Ferrari, A.; Avouris, P.; Steiner, M. Electroluminescence in single layer MoS$_2$. *Nano Lett.* **2013**, *13*, 1416−1421.

(12) Chhowalla, M.; Shin, H. S.; Eda, G.; Li, L.-J.; Loh, K. P.; Zhang, H. The chemistry of two-dimensional layered transition metal dichalcogenide nanosheets. *Nat. Chem.* **2013**, *5*, 263−275.

(13) Yu, J.; Li, J.; Zhang, W.; Chang, H. Synthesis of high quality two-dimensional materials via chemical vapor deposition. *Chem. Sci.* **2015**, *6*, 6705−6716.

(14) Chen, J.; Tang, W.; Tian, B.; Liu, B.; Zhao, X.; Liu, Y.; Ren, T.; Liu, W.; Geng, D.; Jeong, H. Y. Chemical Vapor Deposition of High-Quality Large-Sized MoS$_2$ Crystals on Silicon Dioxide Substrates. *Adv. Sci.* **2016**, *3*, 1500033.

(15) Zhan, Y.; Liu, Z.; Najmaei, S.; Ajayan, P. M.; Lou, J. Large-area vapor-phase growth and characterization of MoS$_2$ atomic layers on a SiO$_2$ substrate. *Small* **2012**, *8*, 966−971.

(16) Najmaei, S.; Liu, Z.; Zhou, W.; Zou, X.; Shi, G.; Lei, S.; Yakobson, B. I.; Idrobo, J.-C.; Ajayan, P. M.; Lou, J. Vapor phase growth and grain boundary structure of molybdenum disulfide atomic layers. *Nat. Mater.* **2013**, *12*, 754−759.

(17) Jeon, J.; Lee, J.; Yoo, G.; Park, J.-H.; Yeom, G. Y.; Jang, Y. H.; Lee, S. Size-tunable synthesis of monolayer MoS$_2$ nanoparticles and their applications in non-volatile memory devices. *Nanoscale* **2016**, *8*, 16995−17003.

(18) Sun, L.; Leong, W. S.; Yang, S.; Chisholm, M. F.; Liang, S. J.; Ang, L. K.; Tang, Y.; Mao, Y.; Kong, J.; Yang, H. Y. Concurrent Synthesis of High-Performance Monolayer Transition Metal Disulfides. *Adv. Funct. Mater.* **2017**, *27*, 1605896.

(19) Weber, T.; Muijsers, J.; Van Wolput, J.; Verhagen, C.; Niemantsverdriet, J. Basic reaction steps in the sulfidation of crystalline MoO$_3$ to MoS$_2$, as studied by X-ray photoelectron and infrared emission spectroscopy. *J. Phys. Chem.* **1996**, *100*, 14144−14150.

(20) Kumar, P.; Singh, M.; Sharma, R. K.; Reddy, G. Reaction mechanism of core−shell MoO$_2$/MoS$_2$ nanoflakes via plasma-assisted sulfurization of MoO$_3$. *Mater. Res. Express* **2016**, *3*, 055021.

(21) Shi, X.-R.; Wang, J.; Hermann, K. Theoretical cluster studies on the catalytic sulfidation of MoO$_3$. *J. Phys. Chem. C* **2010**, *114*, 6791−6801.

(22) Manikandan, P.; Carter, J. A.; Dlott, D. D.; Hase, W. L. Effect of carbon chain length on the dynamics of heat transfer at a gold/hydrocarbon interface: comparison of simulation with experiment. *J. Phys. Chem. C* **2011**, *115*, 9622−9628.

(23) Segall, D. E.; Strachan, A.; Goddard, W. A.; Ismail-Beigi, S.; Arias, T. A. Ab initio and finite-temperature molecular dynamics studies of lattice resistance in tantalum. *Phys. Rev. B: Condens. Matter Mater. Phys.* **2003**, *68*, 014104.

(24) Zheng, M.-J.; Szlufarska, I.; Morgan, D. Ab initio prediction of threshold displacement energies in ZrC. *J. Nucl. Mater.* **2016**, *471*, 214−219.

(25) Yadav, V. K.; Klein, M. L. Probing the dynamics of N-methylacetamide in methanol via ab initio molecular dynamics. *Phys. Chem. Chem. Phys.* **2017**, *19*, 12868−12875.

(26) Tokarz-Sobieraj, R.; Hermann, K.; Witko, M.; Blume, A.; Mestl, G.; Schlögl, R. Properties of oxygen sites at the MoO$_3$(010) surface: density functional theory cluster studies and photoemission experiments. *Surf. Sci.* **2001**, *489*, 107−125.

(27) Coquet, R.; Willock, D. J. The (010) surface of α-MoO$_3$, a DFT + U study. *Phys. Chem. Chem. Phys.* **2005**, *7*, 3819−3828.

(28) Hong, S.; Krishnamoorthy, A.; Rajak, P.; Tiwari, S.; Misawa, M.; Shimojo, F.; Kalia, R. K.; Nakano, A.; Vashishta, P. Computational Synthesis of MoS$_2$ Layers by Reactive Molecular Dynamics Simulations: Initial Sulfidation of MoO$_3$ Surfaces. *Nano Lett.* **2017**, *17*, 4866−4872.

(29) Wang, L.; Maxisch, T.; Ceder, G. Oxidation energies of transition metal oxides within the GGA + U framework. *Phys. Rev. B: Condens. Matter Mater. Phys.* **2006**, *73*, 195107.

(30) Perdew, J. P.; Burke, K.; Ernzerhof, M. Generalized gradient approximation made simple. *Phys. Rev. Lett.* **1996**, *77*, 3865−3868.

(31) Henkelman, G.; Uberuaga, B. P.; Jónsson, H. A climbing image nudged elastic band method for finding saddle points and minimum energy paths. *J. Chem. Phys.* **2000**, *113*, 9901−9904.